Research in Astron. Astrophys. Vol.0 (20xx) No.0, 000–000 http://www.raa-journal.org http://www.iop.org/journals/raa (LTFX: yeye.tex; printed on November 18, 2025; 3:18)

 $m{R}$ esearch in $m{A}$ stronomy and $m{A}$ strophysics

Received 20xx month day; accepted 20xx month day

Key words: cosmology: observations — dark ages, reionization, first stars — techniques: image processing — methods: data analysis — methods: statistical

Constraining the Neutral Hydrogen Fraction from SKA Simulated Observation using a Double-Gaussian Decomposition Technique

Jiajun Zhang^{1,2}, Huanyuan Shan^{1,2}

- 1 Shanghai Astronomical Observatory, Chinese Academy of Sciences, China;
- 2 Key Laboratory of Radio Astronomy and Technology, Chinese Academy of Sciences, 20A Datun Road, Chaoyang District, Beijing 100101, China jjzhang@shao.ac.cn

Abstract The Epoch of Reionization (EoR) is a unique phase in cosmic history, marked by the ionization of neutral hydrogen by the first luminous sources. The global neutral hydrogen fraction (x_{HI}) is a key observable for probing this era. This paper presents a novel, statistically robust method to extract the evolution of x_{HI} from the challenging noise-dominated data from the Square Kilometre Array (SKA) Data Challenge 3b, Our approach is based on a key physical insight: the pixel value distribution in SKA intensity maps is a mixture of signals from ionized and neutral regions. We model this distribution as a superposition of two Gaussian components—one fixed at zero representing noise and ionized bubbles, and a second, offset Gaussian tracing the neutral hydrogen signal. We perform this decomposition on data grouped into three redshift bins. The double-Gaussian model provides an excellent fit to the pixel histogram data. The derived x_{HI} values show a clear decreasing trend across the three redshift bins, consistent with a progressing reionization process. And the results are consistent with the provided simulation data. This method offers a powerful, model-independent, and fully interpretable way for measuring x_{HI} from 21 cm data, demonstrating significant potential for application to future SKA observations.

1 INTRODUCTION

Within several million years following the Big Bang, the complex architecture of the cosmic web started to assemble as a consequence of dark matter collapsing under its own gravity. During this era, the initial stellar and galactic systems emerged, whose radiative output progressively ionized the neutral baryonic gas. This phase, termed cosmic reionization, constituted a fundamental transition in the Universe's history, paving the way for the rich variety of structures and astrophysical objects seen today (see, e.g., (Morales & Wyithe 2010) for a detailed overview).

To this day, the cosmic Dark Ages and the subsequent reionization era represent compelling and still largely uncharted chapters in our knowledge of post-Cosmic Microwave Background (CMB) evolution. Deeper exploration and progress in observational methods—such as the deployment of advanced telescope arrays and high-precision measurement capabilities—are crucial for understanding the young universe.

2 Jiajun Zhang

The 21 cm spectral line, originating from the hyperfine splitting of neutral hydrogen's ground state, provides a vital observational window into the Universe throughout the reionization epoch (Pritchard & Loeb 2012). This signal, often called the EoR signal, has been redshifted into the low-frequency radio domain, typically observed between approximately 50 MHz and 200 MHz. To access this signal, several radio interferometric facilities have been developed or proposed, such as the Square Kilometre Array (SKA, (Dewdney et al. 2009)), the Hydrogen Epoch of Reionization Array (HERA, (Abdurashidova et al. 2022)), the Low-Frequency Array (LOFAR, (van Haarlem et al. 2013)), the Murchison Widefield Array (MWA, (Wayth et al. 2018)), the 21 Centimeter Array (21CMA, (Wu 2009)), and the Precision Array for Probing the Epoch of Reionization (PAPER, (Backer et al. 2007)).

Of these instruments, the SKA-Low array represents one of the most ambitious initiatives, with physical construction now underway. It is expected to achieve exceptional sensitivity and angular resolution, positioning it as a leading facility for the probable detection of the EoR signal. SKA Observatory launched a series of data challenges to attract scientists worldwide to participate in detecting the EoR signal. The data challenge that calls for scientists to propose methods to remove foreground has concluded (Bonaldi et al. 2025)¹. Another challenge is to estimate the neutral hydrogen fraction x_{HI} from simulations. Several methods were proposed to estimate x_{HI} from EoR 21cm power spectrum(Liu et al. 2025; González-Hernández et al. 2025). In this paper, we would like to propose a fast method to calculate the x_{HI} from imaging data with good interpretability.

We present the data and methodology in Sec. 2. The Results are presented in Sec. 3. Finally, we provide the conclusion and discussion in Sec. 4.

2 DATA AND METHODOLOGY

2.1 SKA Data Challenge 3b Data

SKA Observatory launched the second phase of Data Challenge 3 (SDC3b) in late 2024 and concluded the results collection at the end of May 2025. This data challenge provided both brightness temperature power spectrum data and imaging data generated from simulations that replicate real observations with SKA-Low. The imaging data include the 21 cm signal from the Epoch of Reionization, residual foreground contamination, and noise corresponding to 1000 hours of observation. The data cover the full frequency range from 151 MHz to 196 MHz, divided into 450 frequency bands. Each band contains an image with 2048×2048 pixels. The data are provided in FITS format and are available on the SDC3b website². The goal of the inference task is to estimate the neutral hydrogen fraction ($x_{\rm HI}$) at three frequency bands and to provide the associated uncertainty. The cosmological and astrophysical model parameters are model-dependent. Estimating the evolution of the neutral fraction serves as a fundamental basis for model-independent analysis of the Epoch of Reionization.

2.2 Data Pre-processing

Figure 1 illustrates the images at 161 MHz, 176 MHz, and 191 MHz, with the color scale representing luminosity. Two key features are evident: first, the highest values are concentrated in the central region rather than the outskirts; second, while the pixel values in the outskirts appear randomly distributed, the central region exhibits coherent structures. As these images are generated from simulated interferometric data lacking a monopole component, the mean pixel value is approximately zero. The primary synthesized beam, formed by the SKA-Low antennas prior to interferometry, is represented by the central region of the images. It is therefore advisable to extract this central region prior to analysis. We extract a circular region with a radius of 400 pixels, applying the same area across all frequency channels.

https://sdc3.skao.int/challenges/foregrounds

² https://sdc3.skao.int/challenges/inference

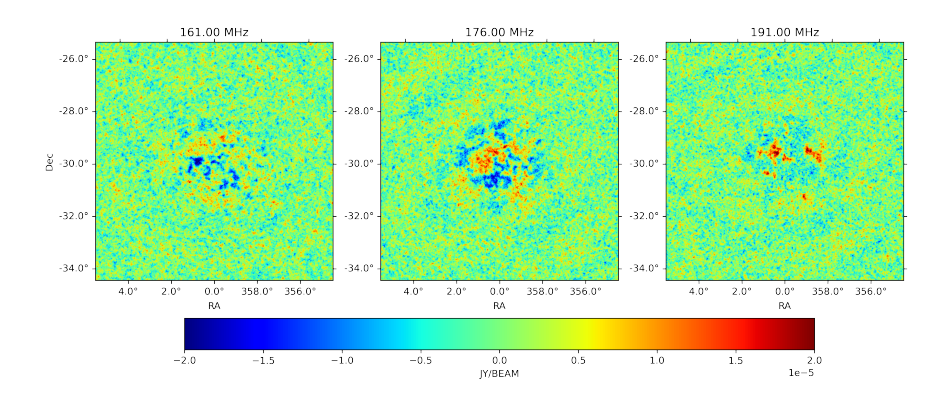


Fig. 1: Three example images from SDC3b, showing the luminosity distribution in the unit of Jy/beam, at 161MHz, 176MHz, and 191MHz. Structured patterns can be seen in the central region.

2.3 The Physical Basis for the Double-Gaussian Model

Under ideal conditions, free from foreground contamination and thermal noise, the 21cm brightness temperature map would directly trace the neutral hydrogen distribution. In this scenario, ionized regions would exhibit no signal beyond the Cosmic Microwave Background (CMB). A reasonable assumption is that the underlying 21cm signal follows a Gaussian distribution with a non-zero mean, reflecting the large-scale structure. In contrast, the combined effect of foreground removal residuals and thermal noise is also commonly modeled as a Gaussian distribution, but one centered at zero, as these components do not correlate with the cosmological signal.

Consider two independent groups of pixels:

- All zeros, represent the reionized pixels.
- Values drawn from a Gaussian distribution $Y \sim \mathcal{N}(\mu_y, \sigma_y^2)$, represent the EoR signal pixels.

Both groups are added to a Gaussian random variable $X \sim \mathcal{N}(0, \sigma_x^2)$, which is independent of Y, represents the noise component (foreground removal residual and thermal noise). After adding X:

- For reionized pixels, the values become X + 0 = X, so the distribution is $N_1 \sim \mathcal{N}(0, \sigma_x^2)$.
- For EoR signal pixels, the values become X + Y, and since X and Y are independent, the distribution is $N_2 \sim \mathcal{N}(\mu_y, \sigma_x^2 + \sigma_y^2)$.

 N_1 is the number of reionized pixels and N_2 is the number of EoR signal pixels. The total number of pixels is $N = N_1 + N_2$. The overall data set is a mixture of two Gaussian distributions:

$$p(z) = \pi_1 \cdot \mathcal{N}(z \mid 0, \sigma_x^2) + \pi_2 \cdot \mathcal{N}(z \mid \mu_y, \sigma_x^2 + \sigma_y^2)$$

$$\tag{1}$$

where $\pi_1 = \frac{N_1}{N}$ and $\pi_2 = \frac{N_2}{N}$ are the mixing weights, with $\pi_1 + \pi_2 = 1$. Therefore, we can try to fit the pixel values in the image by a double-Gaussian model as follows:

$$N(x) = A_{\rm n} \cdot \exp\left[-\frac{1}{2} \left(\frac{x}{\sigma_{\rm n}}\right)^2\right] + A_{\rm s} \cdot \exp\left[-\frac{1}{2} \left(\frac{x - \mu_{\rm s}}{\sigma_{\rm s}}\right)^2\right],\tag{2}$$

where N(x) represents the pixel count distribution for different pixel value x, A_n and σ_n represent the weight and standard deviation for the noise part (foreground removal residual and thermal noise), A_s, $\mu_{\rm s}$ and $\sigma_{\rm s}$ represent the weight, mean value and standard deviation for the 21cm signal part.

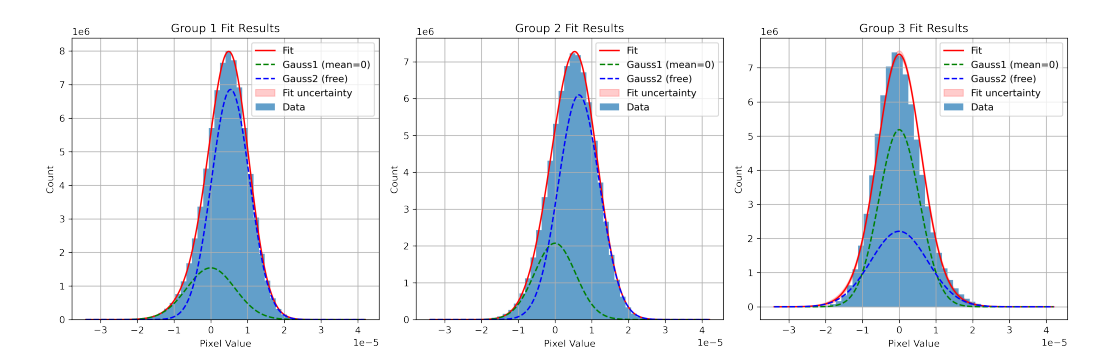


Fig. 2: The histogram and double-Gaussian model fitting results for the pixel values in the images. Group 1 contains 151MHz-166MHz, Group 2 contains 166MHz-181MHz, Group 3 contains 181MHz-196MHz. The green dashed line represents the contribution from foreground removal residual and thermal noise. The blue dashed line represents the contribution from 21cm signal.

2.4 Analysis Pipeline

After fitting, the area under the nonzero-centered Gaussian part represents the number of EoR signal pixels. Divided by the total area under that double-Gaussian, we get the very first estimate of neutral hydrogen fraction x_{HI} . Finally, we should consider that the evolution of x_{HI} being smooth, the bins are chosen not exactly at the frequency required by SDC3b, and the groups are correlated as well. The joint probability distribution is derived through Gaussian Process regression on the binned x_{HI} estimates, modeling the covariance structure across redshift bins to capture the smooth evolution of reionization while accounting for measurement errors.

Given the above consideration, the pipeline can be constructed in the following steps:

- Grouping the data into three redshift bins
- Pick out the central spherical area with a radius of 400 pixels
- Construct the pixel value histograms for each redshift bin
- Performing the non-linear least-squares fit with the double Gaussian model
- Calculating x_{HI} from the ratio of the integrated areas of the Gaussian components
- Propagating fitting errors to estimate uncertainties on x_{HI}
- Calculate the final probability distribution using Gaussian Process regression

3 RESULTS

We have grouped the data of images into three frequency bins, 151MHz-166MHz are grouped as Group 1, 166MHz-181MHz are grouped as Group 2, and 181MHz-196MHz are grouped as Group 3. The histogram of these three groups and the double-Gaussian model fitting are shown in Fig. 2. Note that the green dashed line represents the noise part, which contributes more and more with higher and higher frequency. This is expected because it reflects the larger and larger reionization regions. The fitting results are shown in Tab. 1. And the EoR signal pixel area ratio for Group 1 is 0.7789 ± 0.0059 , for Group 2 is 0.7466 ± 0.0216 , and for Group 3 is 0.3741 ± 0.0335 . Following the pipeline described before, we provide the inference results for these three frequency bins. After Gaussian Process regression, the estimated value of x_{HI} for Group 1 is 0.8092 ± 0.021 , for Group 2 is 0.5883 ± 0.025 , and for Group 3 is 0.1633 ± 0.076 . We illustrate the two-dimensional joint probability results and the one-dimensional probability results in Fig. 3. The one-dimensional probability answer provided by SKA SDC3b is shown in the shaded red region, the red dashed line shows the central value, and the shaded area shows the 1σ region. The inference probability results using our methods are shown in the shaded blue region. It is clear that our method can provide a fast and accurate inference for the x_{HI} value, and the process is

Table 1: Fitting results for three groups of data using the double-Gaussian model. A_n and σ_n represent the amplitude and standard deviation of the Gaussian with fixed mean=0 (reionized pixels), while A_s , μ_s , and σ_s represent the amplitude, mean, and standard deviation of the free Gaussian (EoR signal pixels).

Group	A_n	σ_n	A_s	μ_s	σ_s
				5.386×10^{-6}	
					5.590×10^{-6}
Group 3	5.186×10^{6}	5.519×10^{-6}	2.211×10^{6}	0.000	7.736×10^{-6}

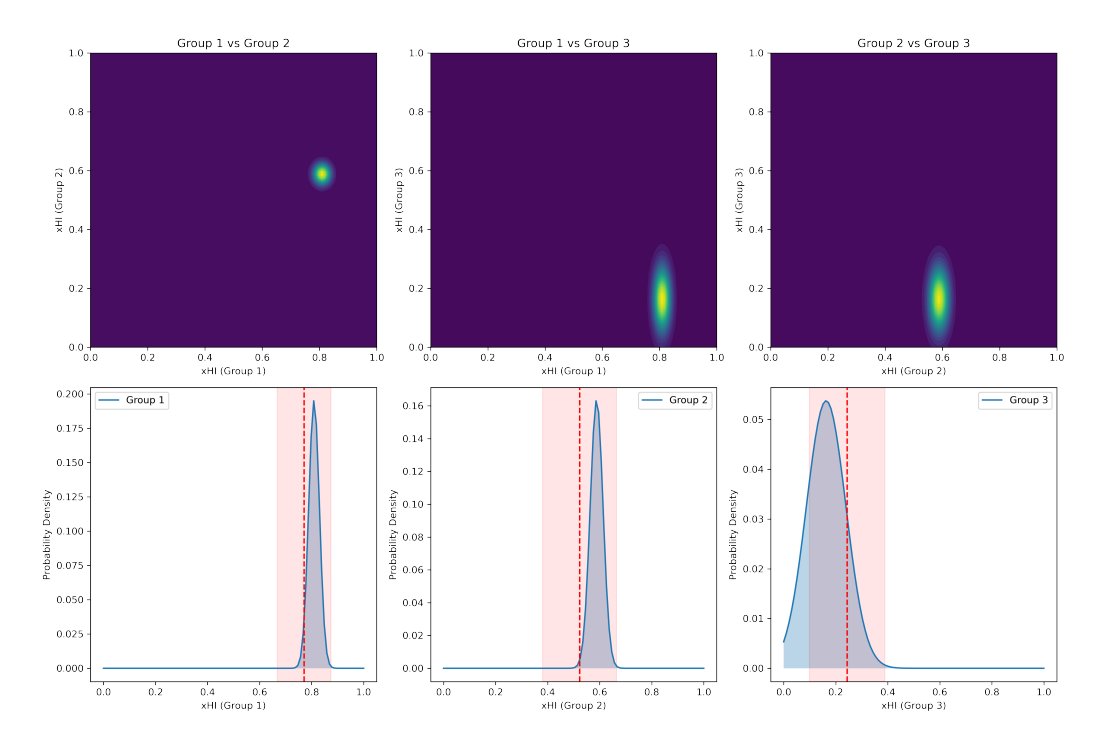


Fig. 3: The top panels show the two-dimensional joint probability for 3 groups of frequency bins. The bottom panels show the one-dimensional probability inference results using our method. The red dashed line is the central value answer, and the shaded red region is the 1σ range, obtained from the SDC3b website.

highly interpretable. Our method is the YEYE team method submitted to SDC3b, with a different choice of binning scheme, resulting in a more precise probability distribution.

4 CONCLUSION AND DISCUSSION

In this paper, we have successfully developed a method to estimate x_{HI} from SKA-like data using a double-Gaussian decomposition, revealing a plausible reionization history. Our method is fast, accurate, and easy to understand. We start from the guessing process when looking at the data images. Turns out that the initial guess and the implementation of the double-Gaussian decomposition method are successful.

We acknowledged that the recent development in machine learning methods application in the field of EoR detection is successful. However, the poor interpretability of the machine learning methods prevents us from understanding the physics behind. Our method looks simple, but useful, and originated

6 Jiajun Zhang

from human intuition. It is interesting to understand how human intuition works, transfer it into logical steps and apply it to our applications.

5 ACKNOWLEDGMENTS

This work is supported by the Ministry of Science and Technology of China (grant No. 2020SKA0110100) and the National Key R&D Program of China No. 2022YFF0504300. This work makes use of data from the SKA Data Challenge 3b. This work is supported by the Specialized Research Fund for State Key Laboratory of Radio Astronomy and Technology.

References

Abdurashidova, Z., Aguirre, J. E., Alexander, P., et al. 2022, ApJ, 925, 221 2

Backer, D. C., Parsons, A., Bradley, R., et al. 2007, in American Astronomical Society Meeting Abstracts, Vol. 211, American Astronomical Society Meeting Abstracts, 133.02 2

Bonaldi, A., Hartley, P., Braun, R., et al. 2025, MNRAS, 543, 1092 2

Dewdney, P. E., Hall, P. J., Schilizzi, R. T., & Lazio, T. J. L. W. 2009, IEEE Proceedings, 97, 1482 2

González-Hernández, D., Wolfson, M., & Hennawi, J. F. 2025, arXiv e-prints, arXiv:2511.02808 2

Liu, Y., de Lera Acedo, E., & Sims, P. 2025, arXiv e-prints, arXiv:2511.10499 2

Morales, M. F., & Wyithe, J. S. B. 2010, ARA&A, 48, 127 1

Pritchard, J. R., & Loeb, A. 2012, Reports on Progress in Physics, 75, 086901 2

van Haarlem, M. P., Wise, M. W., Gunst, A. W., et al. 2013, A&A, 556, A2 2

Wayth, R. B., Tingay, S. J., Trott, C. M., et al. 2018, PASA, 35, e033 2

Wu, X. 2009, in American Astronomical Society Meeting Abstracts, Vol. 213, American Astronomical Society Meeting Abstracts #213, 226.05 2